Journal of Solid State Chemistry 181 (2008) 1876–1881

Contents lists available at ScienceDirect

Journal of Solid State Chemistry

journal homepage: www.elsevier.com/locate/jssc

Photoluminescence in the $Ca_xSr_{1-x}WO_4$ system at room temperature

S.L. Pôrto [a], E. Longo [b], P.S. Pizani [c], T.M. Boschi [c], L.G.P. Simões [d], S.J.G. Lima [e], J.M. Ferreira [a,f], L.E.B. Soledade [a], J.W.M. Espinoza [a], M.R. Cássia-Santos [a], M.A.M.A. Maurera [a], C.A. Paskocimas [g], I.M.G. Santos [a,*], A.G. Souza [a]

[a] Laboratório de Combustíveis e Materiais (LACOM/DQ/CCEN), Universidade Federal da Paraíba, Campus I, Cidade Universitária, João Pessoa, PB, CEP 58059-900, Brazil
[b] CMDMC/LIEC, Instituto de Química, UNESP-Araraquara, Rua Prof. Francisco Degni s/n, Araraquara, SP, CEP 14800-900, Brazil
[c] Departamento de Física, Universidade Federal de São Carlos, São Carlos, Rodovia Washington Luiz km 235, SP, CEP 13565-905, Brazil
[d] Centro Multidisciplinar de Desenvolvimento de Materiais Cerâmicos (LIEC/DQ), Universidade Federal de São Carlos, Rodovia Washington Luiz km 235, São Carlos, SP, CEP 13565-905, Brazil
[e] Laboratório de Solidificação Rápida, Departamento de Tecnologia Mecânica (LSR/DTM/CT), Universidade Federal da Paraíba, Campus I, Cidade Universitária, João Pessoa, PB, CEP 58059-900, Brazil
[f] COAMA, Área de Meio Ambiente, Centro Federal de Educação Tecnológica da Paraíba, Av. 1° de Maio 720, Jaguaribe, João Pessoa, PB, CEP 58015-430, Brazil
[g] Departamento de Engenharia Mecânica, Universidade Federal do Rio Grande do Norte, Natal, RN, CEP 59072-970, Brazil

ARTICLE INFO

Article history:
Received 21 December 2007
Received in revised form
13 March 2008
Accepted 10 April 2008
Available online 30 April 2008

Keywords:
Tungstates
Scheelite
Photoluminescence
Disorder

ABSTRACT

In this work, a study was undertaken about the structural and photoluminescent properties, at room temperature, of powder samples from the $Ca_xSr_{1-x}WO_4$ ($x = 0$–1.0) system, synthesized by a soft chemical method and heat treated between 400 and 700 °C. The material was characterized using Infrared, UV–vis and Raman spectroscopy and XRD. The most intense PL emission was obtained for the sample calcined at 600 °C, which is neither highly disordered (400–500 °C), nor completely ordered (700 °C). Corroborating the role of disorder in the PL phenomenon, the most intense PL response was not observed for pure $CaWO_4$ or $SrWO_4$, but for $Ca_{0.6}Sr_{0.4}WO_4$. The PL emission spectra could be separated into two Gaussian curves. The lower wavelength peak is placed around 530 nm, and the higher wavelength peak at about 690 nm. Similar results were reported in the literature for both $CaWO_4$ and $SrWO_4$.

1. Introduction

Photoluminescence research has been focused on crystalline materials, either pure or doped, mainly with rare earth ions such as Eu^{3+}, Er^{3+}, Nd^{3+}, due to the potential in optical-electronic applications [1].

Nevertheless, photoluminescence (PL) was recently observed in disordered perovskite materials in systems such as $SrTiO_3$ [2,3], $CaTiO_3$ [4], $BaTiO_3$ [5], (Ba,Sr)TiO_3 [6], $PbTiO_3$ [7], $LiNbTiO_3$ [8], $ZrTiO_4$ [9,10], which displayed intense PL emission at room temperature, at the visible region. Such discovery raises a great technological interest, once the crystalline systems need high temperatures for preparation, whereas the disordered systems can be obtained at lower temperatures (below 500 °C), thus reducing the processing cost. Therefore, oxides with low degree of organization are candidates to replace crystalline oxides in a series of optical-electronic applications. Moreover, disordered materials are photoluminescent at room temperature, while the majority of the crystalline materials are only photoluminescent at cryogenic temperatures.

$CaWO_4$ (CWO) is well known for its strong visible luminescence. It has been used for 75 years in X-ray photography as intensifying screen. This is due to its capability to absorb X-rays and convert their energy into radiation, which is able to blacken the photographic film [11]. Conversely, $SrWO_4$ (SWO) does not display room temperature PL. Nowadays the challenge is to use these tungstates as solid-state optoelectronic devices as lasers, optical fibers components or scintillators [12–15].

Cho and Yoshimura [16] investigated the structural evolution and the PL properties, at 77 K, of $Sr_{1-x}Ca_xWO_4$ ($0 \leqslant x \leqslant 1$) films, heat treated from 400 to 1000 °C. Cho et al. [17] also investigated the PL of highly crystalline $CaWO_4$, films at room temperature and at 77 K. These films presented a blue emission at 456 nm (25 °C) and at 465 nm (77 K), with the excitation lines of 254 nm (25 °C) and 251 nm (77 K). The blue emission was ascribed to the WO_3 group defects. Blasse and Schipper [18] studied the PL of barium tungstate and strontium tungstate, both synthesized by solid-state reaction, calcined between 850 and 1100 °C.

Ciaco et al. [1] studied the room temperature PL of amorphous calcium tungstate. Their theoretical calculations results indicate

* Corresponding author. Fax: +55 83 32167441.
E-mail address: ieda@quimica.ufpb.br (I.M.G. Santos).

0022-4596/$ - see front matter © 2008 Elsevier Inc. All rights reserved.
doi:10.1016/j.jssc.2008.04.015

that the formation of threefold coordination in the amorphous system may introduce localized electronic levels in the HOMO and the LUMO, which are related to the formation of the tail observed in the UV–vis spectra.

Orhan et al. [19,20] carried out a joint experimental and theoretical study of the photoluminescence properties of disordered $CaWO_4$ (CWO) thin films and $SrWO_4$ powders. First principles quantum mechanical calculations were employed to study the electronic structure of a crystalline (CWO-c) and an asymmetric (CWO-a) periodic models. The authors related that the symmetry breaking process, on going from CWO-c to CWO-a, creates localized electronic levels above the valence band and that a negative charge transfer process takes place from threefold, $[WO_3]$, to fourfold, $[WO_4]$, tungsten coordinations. As a consequence, polarons are formed in the structure, due to the presence of a disorder–order system. In highly disordered or highly ordered systems, strong polarons are not observed and the photoluminescence vanishes [21].

In this work, a study was undertaken about the structural and photoluminescent properties of powder samples from the $Ca_xSr_{1-x}WO_4$ ($x = 0$, 0.2, 0.4, 0.6, 0.8, 1.0) system, synthesized by the polymeric precursor method and heat treated from 400 to 700 °C.

2. Experimental

The polymeric precursor method [22–26] was used to synthesize $Ca_xSr_{1-x}WO_4$ ($x = 0$, 0.2, 0.4, 0.6, 0.8, 1.0) powders. Tungsten citrate was formed by dissolution of tungstic acid (H_2WO_4) (Vetec—purity 97%) in an aqueous solution of citric acid (Cargil—purity 99%), under constant agitation. Strontium carbonate ($SrCO_3$) (Alfa AESAR—purity 99.99%) and/or calcium carbonate ($CaCO_3$) (Reagen purity 99.66%) were slowly added to the solution. After homogenization, ethylene glycol (Synth—purity 99.5%) was added to promote the citrate polymerization by the polyesterification reaction. The molar ratio between citric acid and the sum of metals was 3:1. The citric acid/ethylene glycol mass ratio was fixed as 60:40.

After the primary heat treatment at 300 °C, the powders were primarily heated at 300 °C for 24 h and then at temperatures ranging from 400 to 700 °C for 4 h. The final composition was evaluated by X-ray fluorescence (XRF 1800—Shimadzu). The samples were structurally characterized, using XRD and Raman spectroscopy. The morphology was evaluated by FEG-SEM.

The diffraction patterns were recorded in a Siemens D-5000 diffractometer, using the Fe$K\alpha$ radiation source. The Raman spectra were taken with a Bruker model RFS/100/S FT-Raman spectrometer, using the 1064 nm line of a Nd:YAG laser, with a 60 mW power.

Field-emission scanning electron microscopy (FEG-SEM) (FEI-Sirion), using a lens secondary electron detector, was used to observe the microstructure of the powders.

The spectral dependence of optical absorbance for the $Ca_xSr_{1-x}WO_4$ powders, heat treated at different temperatures, was measured in the wavelength range from 200 to 800 nm, using a Cary 5G spectrophotometer.

The PL spectra of the $Ca_xSr_{1-x}WO_4$ powder samples were taken with a U1000 Jobin-Yvon double monochromator coupled to a cooled GaAs photomultiplier and a conventional photon counting system. The 488.0 nm exciting wavelength of an argon ion laser was used, with the output power of 60 mW. A cylindrical lens was used to prevent the sample from overheating. The slit width was 100 μm. All the measurements were taken at room temperature.

3. Results

The photoluminescence results of the system $Ca_xSr_{1-x}WO_4$ are presented in Fig. 1. These results were evaluated as a function of the heat treatment temperature and the Ca/Sr molar ratio.

In relation to temperature, it can be clearly noticed that the maximum PL intensity was obtained for the sample heat treated at 600 °C. A significantly lower PL was seen for the sample heat treated at 500 °C, whereas the heat treatment temperatures of 400 and 700 °C yielded small PL intensities. It may be observed that the sample $Ca_{0.6}Sr_{0.4}WO_4$ presents the highest PL intensity, indicating that the use of two different modifiers leads to an increase in the PL intensity. According to XRF results, the real composition of this sample is $Ca_{0.6}Sr_{0.45}W_{0.95}O_4$.

In order to identify the reasons for this behavior, the samples were characterized by Raman and UV–vis spectroscopy (Figs. 2 and 3), X-ray diffraction (Figs. 4 and 5) and FEG-SEM (Fig. 6).

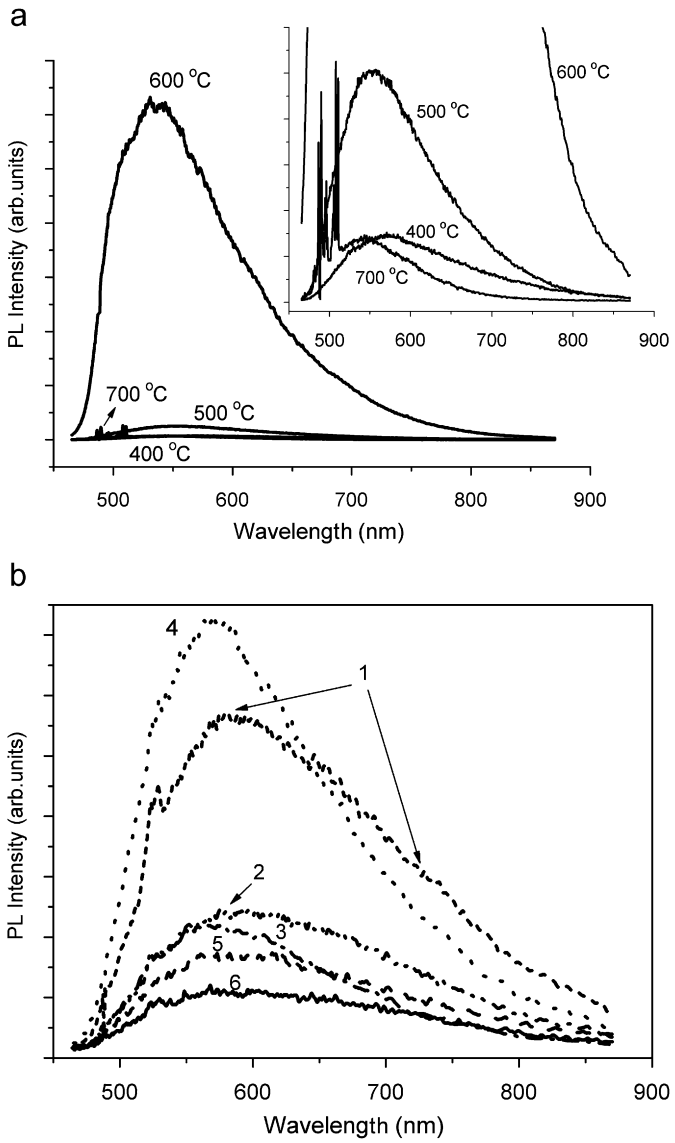

Fig. 1. (a) PL spectra of the $Ca_{0.6}Sr_{0.4}WO_4$ samples heat treated at different temperatures. The inset shows the magnification of the PL spectra, with emphasis in the PL emission after calcination at 400, 500 and 700 °C; (b) PL spectra of the $Ca_xSr_{1-x}WO_4$ samples ($x = 0$–1) heat treated at 400 °C for 4 h. Legend: 1—$SrWO_4$, 2—$Ca_{0.2}Sr_{0.8}WO_4$, 3—$Ca_{0.4}Sr_{0.6}WO_4$, 4—$Ca_{0.6}Sr_{0.4}WO_4$, 5—$Ca_{0.8}Sr_{0.2}WO_4$, 6—$CaWO_4$.

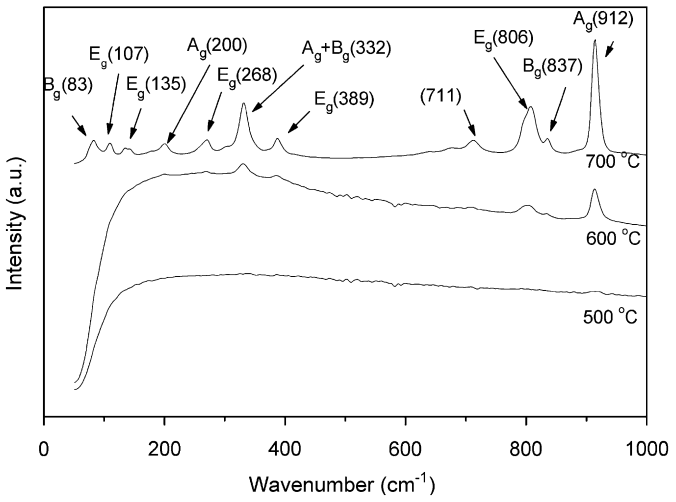

Fig. 2. Raman spectra of the $Ca_{0.6}Sr_{0.4}WO_4$ sample, as a function of temperature.

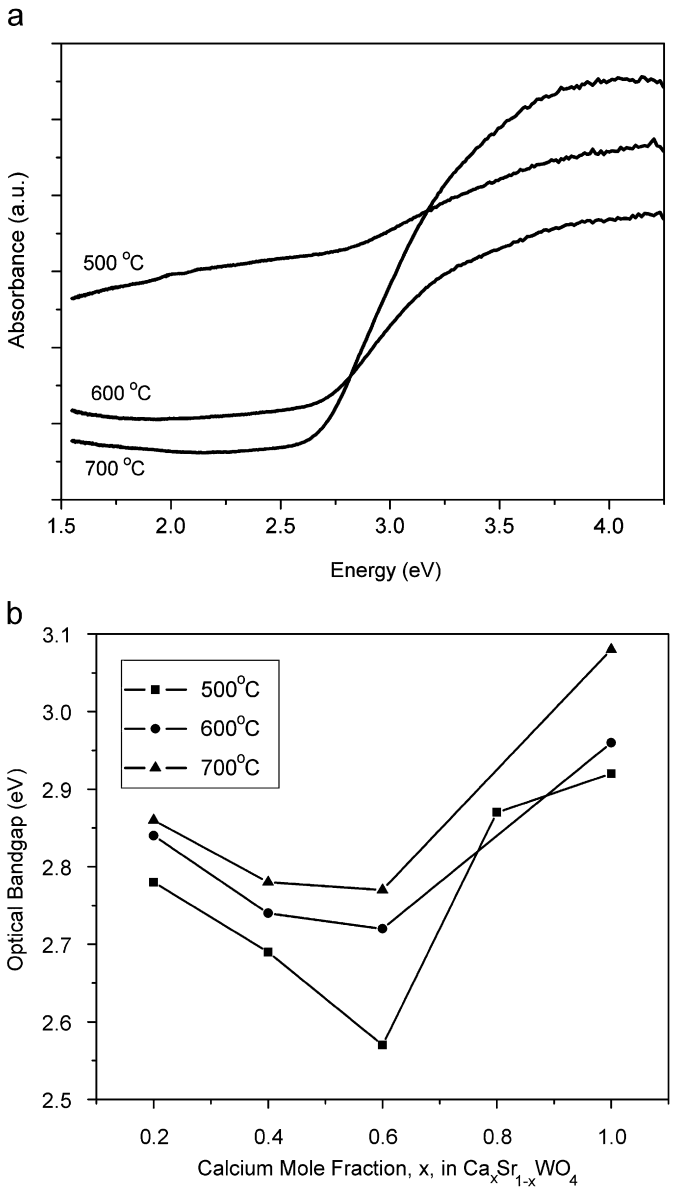

Fig. 3. (a) Absorbance of $Ca_{0.6}Sr_{0.4}WO_4$ powders heat treated at 500, 600 and 700 °C; (b) influence of composition and heat treatment temperature on the optical bandgaps of the samples.

In Fig. 2, the Raman spectra of the $Ca_{0.6}Sr_{0.4}WO_4$ samples heat treated at 500, 600 and 700 °C for 4 h are showed. No vibration mode is noticed at 500 °C. At 600 °C, the peaks at 332 ν_2 (A_g+B_g), 799 for ν_3 (E_g) and 919 cm^{-1} for ν_1 (A_g) are the first ones to appear and are related to the WO_4 groups [27–30]. These peaks indicate the onset of short range order, in the network former region. The samples heat treated at 700 °C display vibration modes at 83 (B_g), 107 (E_g), 135 (E_g), 200 (A_g), 268 (E_g), 332 (A_g+B_g), 389 (E_g), 806 (E_g), 837 (B_g) and 912 cm^{-1} (A_g). The additional vibration mode at 711 cm^{-1} could not be identified, as it was not cited in the literature. These experimental values are in agreement with the values reported by Pontes et al. [27], Basiev et al. [28], Desgreniers et al. [29] and Hardcastle et al. [30].

These results are confirmed by the UV–vis spectra, which show the decrease of the Urbach tail with the temperature increase (Fig. 3a). It can be noted that from 400 to 600 °C, the absorbance increases sharply, followed by a slight decrease from 600 to 700 °C. The samples heat treated at 500 and 600 °C showed a spectral dependence on absorbance similar to that found in amorphous semiconductors, such as amorphous silicon (Si) and insulators, with the presence of exponential optical edges and tails. The nature of these exponential optical edges and tails may be associated with localized defect states promoted by the disordered structure. It can be observed that the absorbance spectra indicate that the sample heat treated at a lower temperature displays a more disordered structure. On the other hand, the sample heat treated at 700 °C showed an interband transition, typical of crystalline materials. The sample heat treated at 400 °C presented high absorbance values throughout the whole photon energy range, due to the presence of a high amount of carbonaceous materials.

As a consequence of the short range disorder, an increase in the bandgap values [31] with temperature occurs (Fig. 3b). In relation to the composition, it can be observed that, for all the heat treatment temperatures, the bandgap values reach a minimum for the composition $Ca_{0.6}Sr_{0.4}WO_4$.

Fig. 4a shows the XRD patterns of the $Ca_{0.6}Sr_{0.4}WO_4$ powders after calcination at several temperatures, while Fig. 4b shows the XRD patterns of samples after calcination at 700 °C. A similar behavior was observed for all the different compositions investigated. A diffuse XRD pattern is observed at 400 °C, indicating the formation of an inorganic disordered phase. The increase of temperature favors the long range order, eliminating structural defects.

In the XRD patterns of the samples calcined at 500 °C, the presence of a crystalline phase was clearly observed, identified by the presence of several broad peaks. With the temperature increase, a better definition of the diffraction peaks is observed. Peaks were indexed to the tetragonal scheelite unit cell (space group $I4_1/a$), according to the JCPDS 41-1431 file, for $CaWO_4$ and JCPDS 8-490 for $SrWO_4$.

According to Fig. 4b, a shift in the XRD peak is observed as calcium substitutes strontium in the lattice. This behavior is due to the change in the lattice parameter. It should be observed that the profiles of the XRD patterns are the same suggesting the formation of a substitutional solid solution, without a change in the crystalline structure, with XRD patterns typical of a single phase system.

For pure $CaWO_4$ and $SrWO_4$, the experimental values of the parameters a and c, as well as the unit cell volume (Fig. 5), were smaller than the values of the respective JCPDS files (312.63 $Å^3$ for

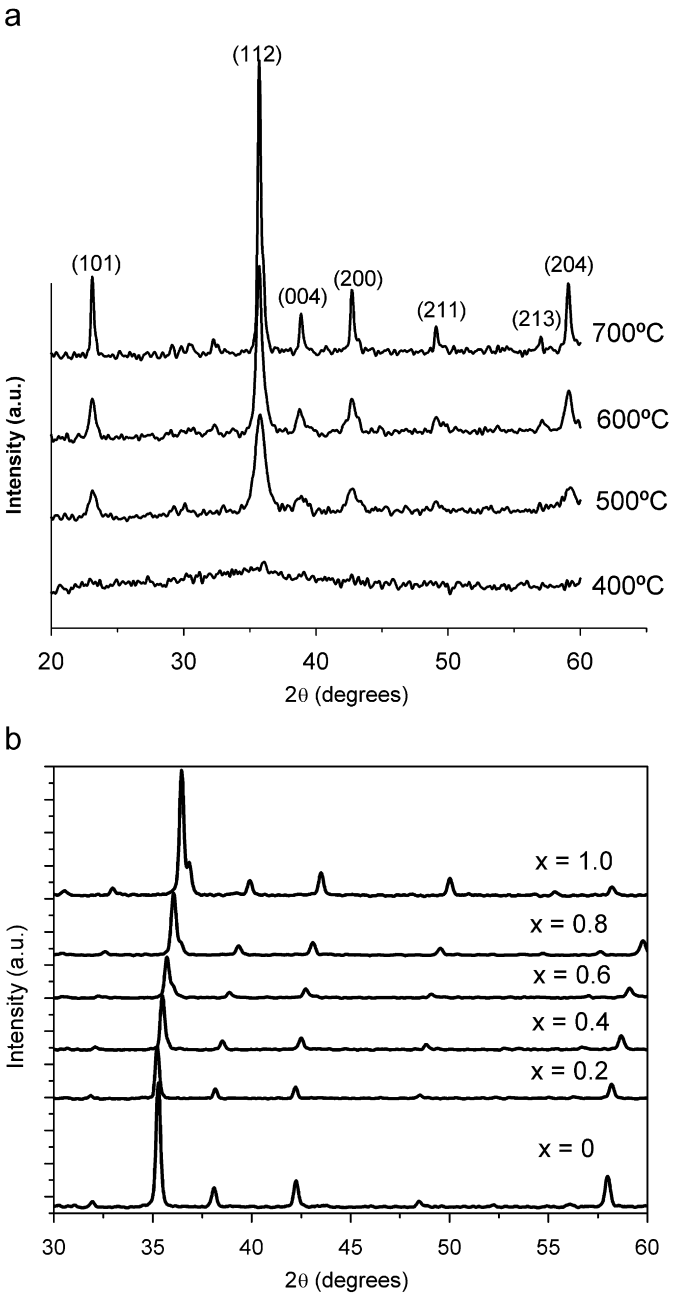

Fig. 4. (a) XRD patterns of the sample $Ca_{0.6}Sr_{0.4}WO_4$ calcined at different temperatures; (b) XRD patterns of the $Ca_xSr_{1-x}WO_4$ system ($x = 0$–1) heat treated at 700 °C.

$CaWO_4$ and 350.66 Å^3 for $SrWO_4$), indicating that a lower amount of defects may be present.

The XRD results were used to calculate the relative crystallinity (Table 1) [22], which is much smaller in the range of x varying from 0.2 to 0.8, than for pure $CaWO_4$ and $SrWO_4$. This suggests that crystallization of $Ca_xSr_{1-x}WO_4$ system is more difficult when Ca^{2+} and Sr^{2+} are simultaneously present in the lattice. The analysis of the unit cell volume points out that the sample with $x = 0.6$ presents the highest deviation from the Vegard Law (Fig. 5).

Values of full width at half maximum (FWHM) were calculated for the (112) peak of the XRD patterns and for the ν_1 (A_g) peak of the Raman spectra (Table 1). Both results indicate that the samples with $x = 0.6$ and 0.8 present the highest disorder, moreover after heat treatment at 600 and 700 °C. These results

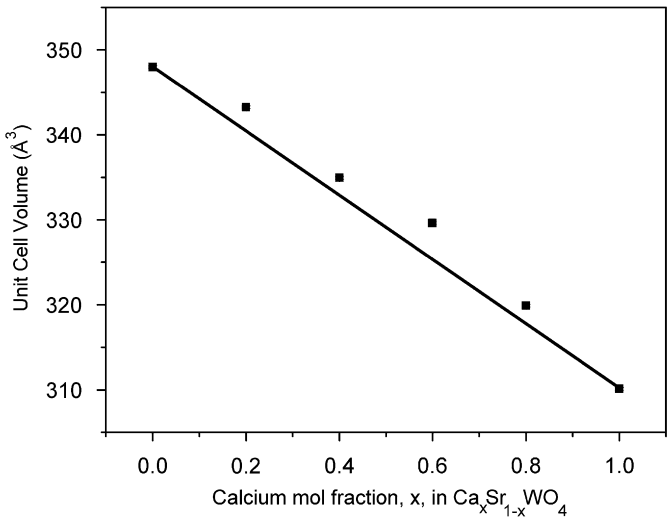

Fig. 5. Deviation from the Vegard Law observed for the variation of the unit cell volume, as a function of calcium mole fraction (x), for the samples calcined at 600 °C.

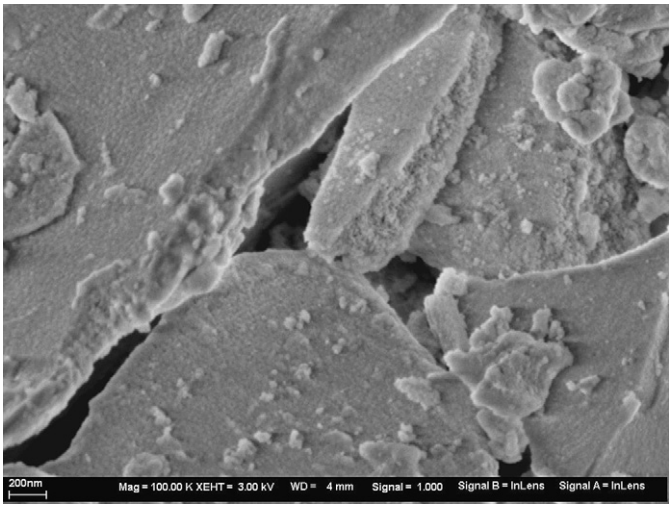

Fig. 6. FEG-SEM micrograph of $CaWO_4$ calcined at 500 °C.

Table 1
Values of FWHM for XRD patterns and Raman spectra, for samples calcined at 600 °C

Sample	FWHM		Relative crystallinity (%)
	XRD (deg)	Raman (cm^{-1})	
$SrWO_4$	0.28 ± 0.01	10.4 ± 0.1	100.0 ± 0.2
$Ca_{0.2}Sr_{0.8}O_4$	0.35 ± 0.01	11.9 ± 0.1	15.9 ± 0.3
$Ca_{0.4}Sr_{0.86}O_4$	0.35 ± 0.01	12.8 ± 0.6	8.4 ± 0.2
$Ca_{0.6}Sr_{0.4}O_4$	0.52 ± 0.01	15.4 ± 0.5	5.3 ± 0.1
$Ca_{0.8}Sr_{0.2}O_4$	0.48 ± 0.01	13.2 ± 0.2	15.2 ± 0.3
$CaWO_4$	0.38 ± 0.01	13.1 ± 0.4	30.6 ± 0.6

indicate that samples with the concomitant presence of two modifiers present a higher amount of disordered material and their crystals present a higher disorder at short and long ranges.

The FEG-SEM micrograph (Fig. 6) shows that samples present a high degree of sintering, even after calcination at 500 °C. This result is related to the high amount of carbon which is not eliminated, even after calcination at 300 °C for 24 h. This organic material is only eliminated by combustion reaction at higher

temperatures, which is highly exothermic, leading to a high amount of energy release. As a consequence, a local increase of temperature occurs, and the particles are sintered.

In FEG-SEM micrographs, crystallites may also be observed, displaying an average size of about 12 nm. This result is in agreement with the crystallite size calculated by the XRD patterns, using the Scherrer equation. For calcium tungstate calcined at 500 °C, a crystallite size of about 17 nm was obtained. Thus, in the present work, micrometric particles were obtained, with nanometric crystallites. As a consequence, nano properties do not affect the photoluminescence.

4. Discussion

As explained by Blasse [11], the PL arises from a radiative return of the excited state to the ground state, phenomenon that is in concurrence with the non-radiative return to the ground state, in which the energy of the excited state is used to excite the vibrations of the host lattice. The radiative emission process occurs more easily if trapped holes or electrons exist in the structure [19].

When the synthesis of tungstates is done using the polymeric precursor method, the structural transformations occurring from disordered to ordered phases start from the early stage of the polyesterification of the citrate solution, containing tungsten and calcium and/or strontium ions. Tungsten, which is the network former, tends ideally to be coordinated by four oxygen atoms. However, before it reaches this ideal configuration there are various coordination numbers, mainly 3 and 4, in the structure. Before the crystallization, i.e. before the heat treatment reaches 700 °C, the $Ca_xSr_{1-x}WO_4$ structure is composed of a random mixture of WO_4 tetrahedra (WO_4 clusters) and WO_3 truncated tetrahedra (WO_3 clusters) linked by the Ca^{2+} and/or Sr^{2+} ions [19–21,32–35].

In the present work, at 400 °C, samples present a high disorder at short and long ranges and no PL emission is observed. At 500 °C, the long range ordering starts, but a very high short range disorder is still observed, with only one small broad peak at 914 cm^{-1} in the Raman spectra and a big Urbach tail. The PL emission increases but it is still very low.

At 600 °C, the Raman spectra present more peaks, all related to WO_4 vibrations, but with low definition and low intensity, whereas the Urbach tails display a further decrease. These results indicate that a higher short range order is observed in the network former region, but the material is not completely ordered, especially when the network modifier region is considered. In the XRD patterns, broad peaks are still observed. These samples present a great increase in the PL emission.

At 700 °C, well defined peaks are observed in the Raman spectra, with an even smaller Urbach tail in the UV–vis spectra. The PL emission vanishes. Comparing the Orhan results with the present work, it may be observed that the higher the heat treatment temperature, the more ordered the structure and the higher the concentration of the WO_4 clusters. When the complete crystallization is reached, only WO_4 clusters exist and the PL drastically decreases, showing that a complete order is not suitable for a good PL emission, similarly to what was previously observed for the case of titanates [6,7,10,36–38] and tungstates [1,19–22]. The best PL emission is obtained for the structure (600 °C) that is neither highly disordered (400 and 500 °C) nor highly ordered (700 °C). Calcinations at higher temperatures would lead to a further increase in the short and long range order, and photoluminescence emission would not occur.

According to the theoretical study of Orhan et al. [19], the charge difference between WO_4 and WO_3 clusters is 0.43 e. This polarization also favors the creation of trapped holes and electrons, giving origin to the room temperature photoluminescence in the investigated powder samples from the $Ca_xSr_{1-x}WO_4$ system. The coexistence of localized levels and this charge gradient creates favorable conditions for the self-trapping of excitons before the emission of luminescence photons [1,19]. Thus, the charge transfer between the WO_4 and WO_3 clusters is related to the presence of ordered and disordered clusters within the microstructure, which are responsible for the photoluminescence emission.

Corroborating the role of order/disorder in the PL phenomenon, the most intense PL response was not observed for pure $CaWO_4$ or $SrWO_4$, but for $Ca_{0.6}Sr_{0.4}WO_4$, which presents the highest amount of disorder. This result is confirmed in all analyses carried out in this work. The FWHM values (Table 1), for samples heat treated at 600 °C, show that the highest short range (Raman data) and long range (XRD data) disorder are observed for this sample. Moreover, this sample has the lowest crystallinity (Table 1), the lowest bandgap (Fig. 3b) and the highest deviation from the Vegard Law (Fig. 5). In spite of the PL emission being related to the presence of WO_4–WO_3 polyhedra, a change of the network modifier region induces a short range disorder in the network former region, increasing photoluminescence.

The PL emission spectra could be separated into three of four Gaussian curves (Table 2). The results were obtained for the sample $Ca_{0.6}Sr_{0.4}WO_4$, heat treated at different temperatures. The peak of highest energy is placed around 2.34 eV, corresponding to 529 nm (green), and the lower energy peak at 1.69 eV, corresponding to 733 nm (red). The other peaks are placed at different regions, according to the heat treatment temperature at 400 and 500 °C, a red emission is observed at 638 and 621 nm, respectively, while an orange emission is observed at 600 and 700 °C, at 590 and 602 nm, respectively.

The values obtained from these Gaussian deconvolution curves agree with the results of other researchers investigating the PL in disordered tungstates. The PL emission observed by Orhan et al. [19] in amorphous $CaWO_4$ thin film can be decomposed into three components: three broad bands at about 530 nm (green), 580 nm (yellow) and 650 nm (red). Orhan et al. [20] also carried out an investigation on the PL in amorphous $SrWO_4$. In this case, two wide bands were observed, at 530 and 600 nm.

In the present work, it may also be observed that the emission energies of all three peaks increase with temperature up to 600 °C, followed by a decrease at 700 °C. This may be related to the higher

Table 2
Deconvolution of the PL spectra of the sample $Ca_{0.6}Sr_{0.4}WO_4$ heat treated at different temperatures

Calcining temperature (°C)	Peak 1		Peak 2		Peak 3		Peak 4	
	Position (nm)	Area (%)	Position (nm)	Area (%)	Position (nm)	Area (%)	Position (nm)	Area (%)
400	–	–	556	46.2	638	30.1	733	23.6
500	–	–	546	54.5	621	29.9	706	15.6
600	502	3.2	529	41.2	590	43.6	693	11.9
700	–	–	534	58.2	602	32.6	704	9.2

short range order in the lattice, leading to higher energy transitions. At 600 °C, one more small peak was necessary to fit the emission band, with energy of 2.47 eV (502 nm), being ascribed to a green emission. For this sample, the highest contribution for the emission band comes from the orange emission, while the other samples have a higher contribution of the green emission.

Orhan et al. [19,20] performed theoretical studies for the disordered structures of $CaWO_4$ and $SrWO_4$, by displacing two tungsten atoms (W*) by 0.3 Å away from oxygen atoms (O*), in order to break the bonds, thus creating truncated WO_3 clusters. In both theoretical studies of tungstates, the authors ascribed the bottom of the conduction band to W* (5*d*) orbitals, whereas the top of the valence band was occupied by O* (2*p*), with the bonded O (2*p*) orbitals lying at a lower energy position within the valence band.

Accordingly, the authors suggest that the presence of various bands in the PL spectra of the CWO thin films is related to these orbitals. The highest energy bands, green and yellow, may be due to the radiative decay occurring from the W* (5*d*) orbitals to the O (2*p*), while the decay corresponding to the lowest energy, red band, would be from W* (5*d*) to O* (2*p*) [19].

5. Conclusions

The polymeric precursor method was successfully employed in the synthesis of powder samples from the $Ca_xSr_{1-x}WO_4$ ($0 \leqslant x \leqslant 1$) system, producing fine single phase powders at a relatively low temperature. A disordered material was obtained for the heat treatment temperatures up to 400 °C. Starting from 500 ºC, the crystallization of the system takes place. The most intense room temperature PL emission (600 °C) was obtained for the structure that is neither highly disordered (400 and 500 °C), nor completely ordered (700 °C).

As for the influence of composition on the optical bandgap, at 600 °C, the highest short and long range disorder was observed for $Ca_{0.6}Sr_{0.4}WO_4$, the same compositions that displayed the highest photoluminescent emission. This result corroborates the role of disorder in the PL phenomenon.

The PL emission spectra could be separated into three of four Gaussian curves, with a red, red/orange and green emission. The lower wavelength peak is placed at around 540 nm, and the higher wavelength peak at about 700 nm. Similar results were reported in the literature for $CaWO_4$.

Acknowledgments

This work was supported by the Brazilian funding programs PRONEX/CNPq/ Fapesq and PADCT/CNPq/MCT.

References

[1] F.R.C. Ciaco, F.M. Pontes, C.D. Pinheiro, E.R. Leite, R.S. Lazarro, J.A. Varela, C.A. Paskocimas, A.G. Souza, E. Longo, Cerâmica 50 (2004) 43–49.
[2] C.D. Pinheiro, E. Longo, E.R. Leite, F.M. Pontes, R. Magnani, J.A. Varela, P.S. Pizani, T.M. Boschi, F. Lanciotti, Appl. Phys. A 77 (2003) 81–85.
[3] L.E.B. Soledade, E. Longo, E.R. Leite, F.M. Pontes, F. Lanciotti, C.E.M. Campos, P.S. Pizani, J.A. Varela, Appl. Phys. A 75 (2002) 629–632.
[4] F.M. Pontes, C.D. Pinheiro, E. Longo, E.R. Leite, S.R. Lazaro, J.A. Varela, P.S. Pizani, T.M. Boschi, F. Lanciotti, Mater. Chem. Phys. 78 (2003) 227–233.
[5] F.M. Pontes, C.D. Pinheiro, E. Longo, E.R. Leite, S.R. Lazaro, R. Magnani, P.S. Pizani, T.M. Boschi, F. Lanciotti, J. Lumin. 104 (2003) 175–185.
[6] E. Longo, E. Orhan, F.M. Pontes, C.D. Pinheiro, E.R. Leite, J.A. Varela, P.S. Pizani, T.M. Boschi, F. Lanciotti, A. Beltrán, J. Andrés, Phys. Rev. B 69 (2004) 125115/1–125115/7.
[7] F.M. Pontes, E.R. Leite, E. Longo, J.A. Varela, P.S. Pizani, C.E.M. Campos, F. Lanciotti, Adv. Mater. Opt. Electr. 10 (2000) 81–89.
[8] Z.R. Silva, J.D.G. Fernandes, D.M.A. Melo, C. Alves, E.R. Leite, C.A. Paskocimas, E. Longo, M.IB. Bernardi, Mater. Lett. 56 (2002) 232–237.
[9] G.F.G. Freitas, R.S. Nasar, M. Cerqueira, D.M.A. Melo, E. Longo, P.S. Pizani, J.A. Varela, Ceram. Int. 29 (2003) 793–799.
[10] G.F.G. Freitas, L.E.B. Soledade, E.R. Leite, E. Longo, P.S. Pizani, T.M. Boschi, C.A. Paskocimas, J.A. Varela, D.M.A. Melo, M. Cerqueira, R.S. Nasar, Appl. Phys. A 78 (2004) 355–358.
[11] G. Blasse, B.C. Grabmaier, Luminescent Materials, Springer, Berlin, Heidelberg, 1994.
[12] M. Nikl, P. Bohacek, E. Mihokova, N. Solovieva, A. Vedda, M. Martini, G.P. Pazzi, P. Fabeni, M. Kobayashi, M. Ishii, J. Appl. Phys. 91 (2002) 5041–5044.
[13] M. Nikl, P. Bohacek, E. Mihokova, M. Kobayashi, M. Ishii, Y. Usuki, V. Babin, A. Stolovich, S. Zazubovich, M. Bacci, J. Lumin. 87 (2000) 1136–1139.
[14] M. Kobayashi, M. Ishii, Y. Usuki, H. Yahagi, Nucl. Instrum. Methods Phys. Res. Sect. A—Accel. Spectrom. Dect. Assoc. Equip. 333 (1993) 429.
[15] M. Nikl, Phys. Status Solidi A 178 (2000) 595–620.
[16] W.S. Cho, M. Yoshimura, J. Appl. Phys. 83 (1998) 518–523.
[17] W.S. Cho, M. Yashima, M. Kakihana, A. Kudo, T. Sakata, M. Yoshimura, Appl. Phys. Lett. 66 (1995) 1027–1029.
[18] G. Blasse, W.J. Schipper, Phys. Status Solidi A 25 (1974) 163–165.
[19] E. Orhan, M.A. Santos, M.A.M.A. Maurera, F.M. Pontes, A.G. Souza, J. Andrés, A. Beltran, J.A. Varela, P.S. Pizani, C.A. Taft, E. Longo, J. Solid State Chem. 178 (2005) 1284–1291.
[20] E. Orhan, M. Anicete-Santos, M.A.M.A. Maurera, F.M. Pontes, C.O. Paiva-Santos, A.G. Souza, J.A. Varela, P.S. Pizani, E. Longo, Chem. Phys. 312 (2005) 1–9.
[21] M. Anicete-Santos, E. Orhan, M.A.M.A. de Maurera, L.G.P. Simões, A.G. Souza, P.S. Pizani, E.R. Leite, J.A. Varela, J. Andrés, A. Beltrán, E. Longo, Phys. Rev. B 75 (2007) 165105/1–165105/11.
[22] D.S. Gouveia, A.G. Souza, M.A.M.A. Maurera, C.E.F. Costa, I.M.G. Santos, S. Prasad, J.G. Lima, C.A. Paskocimas, E. Longo, J. Therm. Anal. Calorim. 67 (2002) 459–464.
[23] D.S. Gouveia, R. Rosenhaim, M.A.M.A. Maurera, S.J.G. Lima, C.A. Paskocimas, E. Longo, A.G. Souza, I.M.G. Santos, J. Therm. Anal. Calorim. 75 (2004) 453–460.
[24] S.L. Porto, M.R. Cassia-Santos, I.M.G. Santos, S.J.G. Lima, L.E.B. Soledade, A.G. Souza, C.A. Paskocimas, E. Longo, J. Therm. Anal. Calorim. 79 (2005) 401–406.
[25] F.M. Pontes, S.H. Leal, M.R.M.C. Santos, E.R. Leite, E. Longo, L.E.B. Soledade, A.J. Chiquito, M.A.C. Machado, J.A. Varela, Appl. Phys. A 80 (2005) 875–880.
[26] S.C. Souza, I.M.G. Santos, M.R.S. Silva, M.R. Cássia-Santos, L.E.B. Soledade, A.G. Souza, S.J.G. Lima, E. Longo, J. Therm. Anal. Calorim. 79 (2005) 451–454.
[27] F.M. Pontes, M.A.M.A. Maurera, A.G. Souza, E. Longo, E.R. Leite, R. Magnani, M.A.C. Machado, P.S. Pizani, J.A. Varela, J. Eur. Ceram. Soc. 23 (2003) 3001–3007.
[28] T.T. Basiev, A.A. Sobol, Y.U.K. Voronko, P.G. Zverev, Opt. Mater. 15 (2000) 205–216.
[29] S. Desgreniers, S. Jandl, C. Carlone, J. Phys. Chem. Solids 45 (1984) 1105–1109.
[30] F.D. Hardcastle, I.E. Wachs, J. Raman Spectrosc. 26 (1995) 397–405.
[31] D.L. Wood, J. Tauc, Phys. Rev. B 5 (1972) 3144–3151.
[32] J.A. Groenink, G. Blasse, J. Solid State Chem. 32 (1980) 9–20.
[33] Z. Lou, M. Cocivera, Mater. Res. Bull. 37 (2002) 1573–1582.
[34] M. Nikl, P. Strakova, K. Nitsch, V. Petricek, V. Mucka, O. Jarolimek, J. Novak, P. Fabeni, Chem. Phys Lett. 291 (1998) 300–304.
[35] M. Martini, G. Spinolo, A. Vedda, M. Nikl, K. Nitsch, V. Hamplova, P. Fabeni, G.P. Pazzi, I. Danei, P. Lecoq, Chem. Phys. Lett. 260 (1996) 418–422.
[36] A.C. Chaves, S.J.G. Lima, R.C.M.U. Araujo, M.A.M.A. Maurera, E. Longo, P.S. Pizani, L.G.P. Simões, L.E.B. Soledade, A.G. Souza, I.M.G. Santos, J. Solid State Chem. 179 (2006) 985–992.
[37] D.M.A. Melo, A. César, A.E. Martinelli, Z.R. Silva, E.R. Leite, E. Longo, P.S. Pizani, J. Solid State Chem. 177 (2004) 670–674.
[38] E.R. Leite, F.M. Pontes, E.C. Paris, C.A. Paskocimas, E.J.H. Lee, E. Longo, P.S. Pizani, J.A. Varela, V. Mastelaro, Adv. Mater. Opt. Electr. 10 (2000) 235–240.